ANNALS OF GEOPHYSICS, 68, SA215, 2025/2026; doi:10.4401/ag-9323
OPEN ACCESS

Evaluating Ionospheric TEC Predictions: A Comparative Analysis between IRI-2016 and IRI-2020 Models Over Indian near Equatorial and EIA Regions During 2016-2018

Mukulika Mondal, Mini Rajput, Jitesh Barman, and Abhay Kumar Singh*

Department of Physics, Institute of Science, Banaras Hindu University, Varanasi-221005, India

Article history: received March 1, 2025; accepted July 25, 2025

Abstract

This study conducts a comprehensive comparative analysis of the ionospheric total electron content (TEC) prediction capabilities of the recent International Reference Ionosphere (IRI) models, specifically IRI-2016 and IRI-2020, by utilizing ground-based GPS measurements over the equatorial ionization anomaly (EIA) region, Varanasi (Geographic: 25.31° N, 82.97° E; geomagnetic: 16.54° N, 157.09° E) and the near equatorial region Bangalore (Geographic: 12.97° N, 77.59° E; geomagnetic: 4.86° N, 150.95° E) during the solar minimum period of 2016-18, corresponding to the 24th solar cycles. Through rigorous statistical evaluations, including diurnal, monthly, seasonal, and annual TEC variation comparison, the root mean squared error (RMSE) of dTEC, and correlation coefficient calculation, this research investigates the forecasting accuracy of Ne-Quick (the default topside option) of IRI-2016, Ne-Quick, and COR2 (the newly added option) of IRI-2020 models. Although the performance of all the topside options is equally good, the Ne-Quick topside of IRI-2016 shows better accuracy over Varanasi (RMSE = 6.09), whereas the prediction by COR2 topside is better over Bangalore (RMSE = 6.02). Furthermore, the overall correlation coefficient analysis highlights the superior performance of the Ne-Quick of the IRI-2016 model (r = 0.88) in capturing GPS TEC dynamics over the near equatorial and low-latitude regions during our study period. However, the performance of all the topside options in forecasting the TEC during the storm time is relatively poor, with a correlation coefficient around ~0.67. These findings offer significant implications for the ionospheric physics research community, providing a validated reference for the IRI models in predicting ionospheric TEC characteristics during solar minimum years over near equatorial and EIA regions.

Keywords: Ionosphere; Total Electron Contents; IRI model; Solar activity; Descending phase; GPS

1. Introduction

Ionospheric electron densities, specifically the total electron content (TEC), are an important parameter in the field of space and ionospheric physics for trans-ionospheric propagation of waves, including radio waves and

GPS signals, hence plays a very significant role in communication, navigation, military, and civilian applications (Rama Rao et al., 2006; Priyadarshi et al., 2025). Due to its immense importance, the empirical model must express electron densities and TEC because ground-based observations are limited and cannot cover the entire globe. Over the past decades, the scientific community has developed many empirical models for predicting the ionospheric TEC. The most recognized model for monitoring the ionosphere is the International Reference Ionosphere (IRI). From its 1st development, the IRI model has been improved and upgraded over time (Bilitza and Reinisch, 2008; Bilitza et al., 2014; Bilitza et al., 2017). The latest available model is the IRI-2020 (Bilitza et al., 2022) model, which is updated by the scientific community from its older version, the IRI-2016 (Bilitza et al., 2017). The topside electron density option Ne-Quick, developed by Nava et al. (2008), was treated as the default option of the IRI-2016 version. A new option for calculating the topside electron density, namely COR2, is added in the IRI-2020 version based on the report of Bilitza and Xiong (2021). The IRI model at any desired location can be used to estimate various ionospheric parameters by choosing the option for height from 60 km to 2000 km. From the IRI model, TEC can be calculated by performing integration of the electron density profile between the lower specified boundary and the user-defined upper boundary. This ionospheric model has variable accuracy over different regions. However, the reliability of the predicted TEC by the IRI models over the equatorial/ low latitude regions is relatively poor in comparison to higher latitudes due to the pronounced Fountain effect or the large temporal and spatial variations of the electron density. In this region, the processes such as the production of ionization by solar extreme ultraviolet radiation, loss through charge exchange with N_2 and O_2, and transport parallel to the geomagnetic field lines through $\mathbf{E} \times \mathbf{B}$ electrodynamical plasma drift are more significant than that at mid and high latitude (Bailey et al., 1997). The north-south geomagnetic field combines with a daytime eastward electric field to produce an upward $\mathbf{E} \times \mathbf{B}$ plasma drift at the geomagnetic equator that initiates the renowned fountain effect, causing further equatorial ionization anomaly (EIA) (Appleton, 1946; Rishbeth, 1972). Therefore, the performance of the IRI model in predicting the ionospheric TEC over such regions is important in comparison to the ground-based GPS observation and the mutual comparison between the two versions of the IRI models.

Comparative studies between ground-based measurements and recent versions (IRI-2016, 2020) of the IRI model over equatorial and low-latitude ionosphere were reported by many researchers. Numerous works have been documented using the IRI-2016 model-derived TEC and its previous version (Rao et al., 2019; Tariq et al., 2019; Endeshaw, 2020; Kumar, 2020; Amaechi et al., 2021; Patari et al., 2021; Nibigira et al., 2021; Ogwala et al., 2021, 2022; Chaurasiya et al., 2023; Sulungu, 2024 and many other references). Tariq et al. (2019) compared IRI-2016 and GPS TEC in Pakistan during 2015-2017. Endeshaw (2020 reported the performance of IRI-2016 over Ethiopia during 2016. Amaechi et al. (2021) reported the IRI-2016 model-derived TEC over the African region. Patari et al. (2021) compared the IRI-2016 model with GPS during 2013-2018 over the EIA region Agartala. Nibigira et al. (2021) analysed the IRI-2016 model TEC during 2016-2018 over the low-latitude ionosphere. Sulungu (2024) compared IRI-2016 TEC with GPS during 2019-2021 over the African region. Kumar et al. (2012) reported a comparative study between GPS and IRI-2007 over Varanasi, Hyderabad, and Bangalore. Rathore et al. (2015) compared the IRI-2012 and GPS observations during 2012-2013 over Varanasi. Kumar et al. (2016) studied the performance of the IRI-2012 model over Lucknow and Bangalore. Rao et al. (2019) studied the comparison between IRI-2016 and GPS over Varanasi during 2008-2018. However, a few works have been reported till now on the validation of the IRI-2020 model performance (Bilitza et al., 2022; He et al., 2023; Marew et al., 2023; Schreiber et al., 2024; Acevedo et al., 2024; Ogwala et al., 2024; Yang et al., 2024). He et al. (2023) and Yang et al. (2024) worked on the performance of the IRI-2020 model using GPS TEC over China. Marew et al. (2023) reported a comparative study between IRI-2016 and IRI-2020 over equatorial latitudes. Schreiber et al. (2024) reported the prediction performance of the COR2 topside option of the IRI-2020 model over 4 low-latitude stations. Acevedo et al. (2024) worked on the TEC prediction over Mexico using the IRI-2020 model. Ogwala et al. (2024) reported the prediction performance of IRI-2016 and IRI-2020 over the African sector during 2016-2021. The previous studies reported discrepancies (overestimation/ underestimation) between the modeled TEC and GPS TEC. This indicates that the validation of the IRI model results needs further investigation.

Despite numerous advancements in ionospheric models, discrepancies between observations and predictions persist, underscoring the need for continual refinement, especially over the Equatorial and EIA regions. To the best of our knowledge, the performance of the latest topside options of the IRI-2020 model in predicting the TEC over the Indian equatorial and EIA region has not yet been reported in the literature during the declining phase of the 24th solar cycle. As the NeQ topside option is considered the default option of the IRI model since the development of the IRI-2012 version (Bilitza et al., 2014; 2017), and the COR2 topside option is the latest addition to the IRI-2020

version, we took these two topside options for our study. In this paper, we explore the variations of ground-based GPS-TEC during different seasons of the decreasing phase of the 24th solar cycle during 2016-2018. GPS-TEC variations during summer, winter, and equinox have been compared with the various topside options of IRI-2016 and IRI-2020 models over the near equatorial region Bangalore (Geographic: 12.97° N, 77.59° E; geomagnetic: 4.86° N, 150.95° E) and EIA region Varanasi (Geographic: 25.31° N, 82.97° E; geomagnetic: 16.54° N, 157.09° E). The aim is to set up a mutual comparative analysis between the three topside formulations: Ne-Quick from IRI-2016 and Ne-Quick and COR2 from IRI-2020 models by comparing their prediction accuracy with ground-based GPS measurements over the near equatorial station Bangalore and the low latitude station Varanasi. Further, we have explored the performance of these three topside options during geomagnetic storms recorded between 2016-2018. The improvement in the IRI-2020 model as compared to its previous version, the IRI-2016 model, was investigated over Bangalore and Varanasi based on rigorous statistical analysis, such as TEC dynamics, correlation coefficient calculation using linear regression analysis, and root mean square error analysis. By highlighting areas of agreement and divergence, our work contributes to the ongoing effort to enhance the IRI model's reliability, ensuring its utility across various scientific and technological fields. This comprehensive approach aims to shed light on the intricate dynamics of the ionosphere, focusing on improving the accuracy and applicability of ionospheric models in real-world scenarios.

2. Data Analysis and Methodology

The IRI model provides TEC values for any given value of longitude, latitude, and time. In our study, we compare the accuracy of the IRI 2016 and IRI-2020 models as compared to ground-based GPS-TEC measurements over the EIA region Varanasi (Geographic: 25.31° N, 82.97° E; geomagnetic: 16.54° N, 157.09° E) and near equatorial region Bangalore (Geographic: 12.97° N, 77.59° E; geomagnetic: 4.86° N, 150.95° E) during the descending phase of the 24th solar cycle, solar minimum periods 2016-2018. IRI model TEC is evaluated using the Ne-Quick topside electron density option from IRI-2016 and the Ne-Quick and COR2 options of IRI-2020. Throughout the paper, Ne-Quick of IRI-2016, Ne-Quick, and COR2 of IRI-2020 are referred to as NeQ-16, NeQ-20, and COR2, respectively.

To evaluate the prediction performance of the IRI model, ten geomagnetic quiet days taken for each month of a year are chosen for our analysis as the IRI model performs better during geomagnetic quiet days. For brevity, we will call the topside electron density options as topside options onwards in this study. All the IRI model data was downloaded from the IRI website: ccmc.gsfc.nasa.gov. using the topside options while keeping the electron density *Ne* of F-peak constant at CCIR. In our study, the slant total electron content (STEC) data is derived from GPS data recorded in RINEX format at the low latitude station Varanasi. The GPS data of Bangalore was downloaded from the IGS website. The STEC estimated from the GPS data is further converted into vertical total electron content (VTEC) by using the following relation given below (Rama Rao et al., 2006)

$$VTEC = \frac{STEC - (b_R + b_S)}{S(\xi)} \text{.....} \quad (1)$$

where b_R and b_S, respectively are the receivers and satellite biases and ξ is the elevation angle measured in degree, is the slant factor or obliquity factor which depends on the zenith angle θ at the Ionospheric Pierce Point (IPP). The expression for the slant factor $S(\xi)$ is given below:

$$S(\xi) = \frac{1}{\cos(\theta)} = \left[\frac{1 - R_E \cos(\xi)}{R_E + h}\right]^{-1/2} \text{.....} \quad (2)$$

where R_E is the Earth's mean radius, and h is the ionospheric effective height above the Earth's surface. Typically, h is taken as 350 km over the Indian region. We have classified the year into three seasons: the summer season (May, June, July, and August), the Winter season (November, December, January, and February), and the Equinox season (March, April, September, and October). The seasonal analysis of VTEC from GPS is carried out and further compared with the IRI model. The TEC data was calculated for seasonal variation analysis by taking the mean of a season or

four months. In addition, we have also analyzed the deviation of IRI-TEC from GPS-TEC (IRI-GPS), represented as dTEC. To calculate the correlation coefficient (r), the following formula is used:

$$r = \frac{\sum_{i=1}^{N}\left(\mathrm{TEC}_i^{\mathrm{GPS}} - \overline{\mathrm{TEC}^{\mathrm{GPS}}}\right)\left(\mathrm{TEC}_i^{\mathrm{Model}} - \overline{\mathrm{TEC}^{\mathrm{Model}}}\right)}{\sqrt{\sum_{i=1}^{N}\left(\mathrm{TEC}_i^{\mathrm{GPS}} - \overline{\mathrm{TEC}^{\mathrm{GPS}}}\right)^2 \sum_{i=1}^{N}\left(\mathrm{TEC}_i^{\mathrm{Model}} - \overline{\mathrm{TEC}^{\mathrm{Model}}}\right)^2}} \tag{3}$$

where $\mathrm{TEC}^{\mathrm{GPS}}$, and $\mathrm{TEC}^{\mathrm{Model}}$ are the TEC data from GPS and the Model, respectively. $\mathrm{TEC}^{\mathrm{GPS/Model}}$ is the average of the TEC data from GPS/Model.

The root mean squared error (RMSE) of dTEC is calculated using the following equation:

$$\mathrm{RMSE} = \sqrt{\frac{1}{N}\sum_{i=1}^{N}\left(\mathrm{TEC}_i^{\mathrm{Model}} - \mathrm{TEC}_i^{\mathrm{GPS}}\right)^2} \tag{4}$$

The best line fitting to the data between the Model and GPS TEC data is done by the least linear regression method using the equation of a line

$$\left.\begin{aligned} \mathrm{TEC}^{\mathrm{Model}} &= \mathrm{intercept} + \mathrm{slope} \times \mathrm{TEC}^{\mathrm{GPS}} \\ \mathrm{slope} &= \frac{\sum_{i=1}^{N}\left(\mathrm{TEC}_i^{\mathrm{GPS}} - \overline{\mathrm{TEC}^{\mathrm{GPS}}}\right)\left(\mathrm{TEC}_i^{\mathrm{Model}} - \overline{\mathrm{TEC}^{\mathrm{Model}}}\right)}{\sum_{i=1}^{N}\left(\mathrm{TEC}_i^{\mathrm{GPS}} - \overline{\mathrm{TEC}^{\mathrm{GPS}}}\right)^2} \\ \mathrm{intercept} &= \overline{\mathrm{TEC}^{\mathrm{Model}}} - \mathrm{slope} \times \overline{\mathrm{TEC}^{\mathrm{GPS}}} \end{aligned}\right\} \tag{5}$$

All the data analysis and plotting are done using Python programming.

3. Results and Observations

3.1 Diurnal and Monthly Variation of TEC

The diurnal variation of TEC of any region is due to solar radiation, which depends mainly on the Earth's rotation around its axis. In the low-latitude ionosphere, electron production by photoionization, electron loss by recombination with neutral atoms, and electron transportation through the fountain effect are the three reasons for the diurnal variation of TEC (Panda et al., 2015). The variation of TEC over Varanasi (cf. Fig. 1) and Bangalore (cf. Fig. 2) during the declining phase of the 24$^{\mathrm{th}}$ solar cycle, 2016-2018, using GPS measurements, are analyzed here. The results were compared with the modeled TEC from IRI-2016 and IRI-2020 using topside options Ne-Quick and COR2.

3.1.1 TEC variation over Varanasi

Figure 1 reveals the diurnal variation of GPS-TEC with IRI-2016 and IRI-2020 modeled TEC of each month of a year over Varanasi during 2016-2018. Hourly mean TEC of each month of a particular year is shown in each row of Fig. 1. For each study year, time in UT (hour) is represented periodically from 0 to 24 for each month along the bottom horizontal axis and months are written along the top horizontal axis, whereas the vertical axis represents the vertical TEC (VTEC) in TECU (1 TECU = 10^{16} electrons/m^2). The variation of TEC derived from options NeQ-16, NeQ-20, COR2, and GPS is shown in blue, green, magenta, and red, respectively, in Fig. 1. These color representations

are kept consistent in all the figures throughout the paper for better clarity. Overall, the diurnal pattern of TEC variation of each month of a specific year shows a similar trend for all topside options of the IRI model taken in our study and GPS over Varanasi. TEC value increases from early morning, reaches a maximum value at around noontime hours, and decays during the afternoon. However, the maximum TEC values vary with the months of a particular year.

For all the study years, the daytime peak TEC values for GPS as well as NeQ-16, NeQ-20, and COR2 show a nearly sinusoidal trend with peaks around April and October and valley regions at January-April, May-August, and September-December. Another common feature observed in Fig. 1 is that the TEC from NeQ-16, NeQ-20, and COR2 topside options overestimates GPS-TEC during the daytime and exhibits nearly identical behavior with GPS-TEC during nighttime throughout all the years (2016-2018). Notably, GPS-TEC slightly overestimates model-derived TEC during the noontime hours. From GPS measurements, the highest TEC values are observed in September (40 TECU), April (33 TECU), and April (30 TECU) for the years 2016, 2017, and 2018, respectively, at around 7 UT-9 UT (12 LT-2 LT). The estimated results by the three possibilities of IRI models (NeQ-16, NeQ-20, and COR2), taken in our study, show good agreement with the GPS TEC for all the study years except 2016, with the maximum TEC found to be in April (~60 TECU).

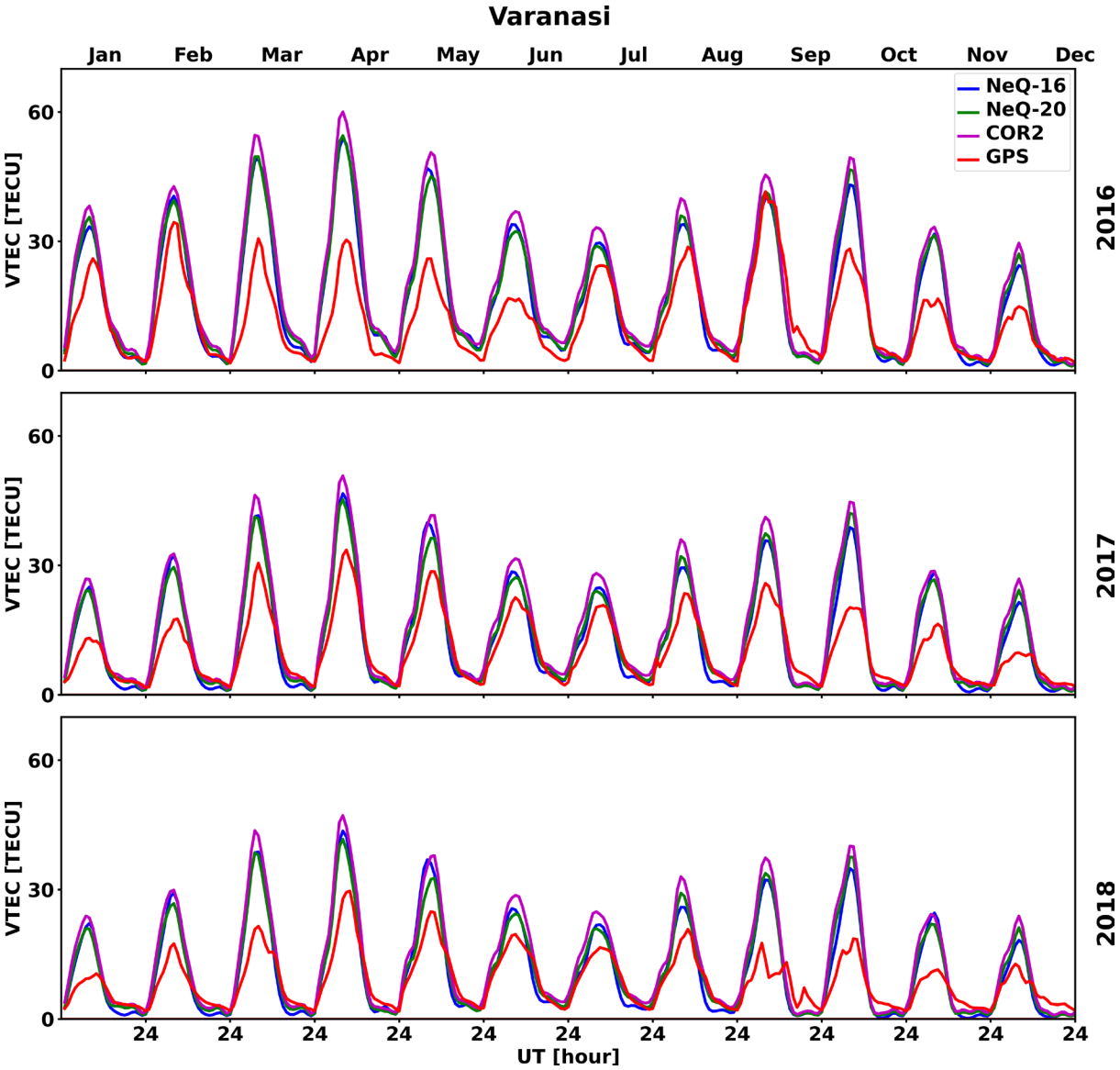

Figure 1. Diurnal variation of hourly TEC averaged over each month from GPS and three topside options (NeQ-16, NeQ-20, COR2) from IRI-2016 and IRI-2020 over Varanasi during 2016-2018.

3.1.2 TEC variation over Bangalore

Figure 2 depicts the diurnal variation of TEC using GPS measurements and the IRI-2016 and IRI-2020 models with three topside options, NeQ-16, NeQ-20, and COR2, during 2016-2018 over Bangalore. All the representations used in Fig. 2 are the same as in Fig. 1.

Overall, in each month of a particular year over Bangalore, TEC from IRI models and GPS exhibits a similar pattern in diurnal variation as observed for Varanasi (see Fig. 1 and Fig. 2) with morning rise, daytime maximum, and afternoon decay. However, in contrast to Varanasi, the increasing rate of TEC in the early morning as well as the rate of decay in the afternoon are much slower in Bangalore, resulting in a broader peak compared to that over Varanasi. Compared to Varanasi, the diurnal peak for Bangalore occurs later at 9 UT-11 UT (14 LT-16 LT). The variation of the highest TEC values of each month exhibits a nearly similar sinusoidal pattern as seen for Varanasi. From GPS measurements, the highest TEC values are observed in March (45 TECU), September (45 TECU), and April (30 TECU) for the years 2016, 2017, and 2018, respectively. On the other hand, the highest TEC from the three topside options of the IRI model shows good agreement with the GPS-TEC with a small deviation of ± 6 TECU.

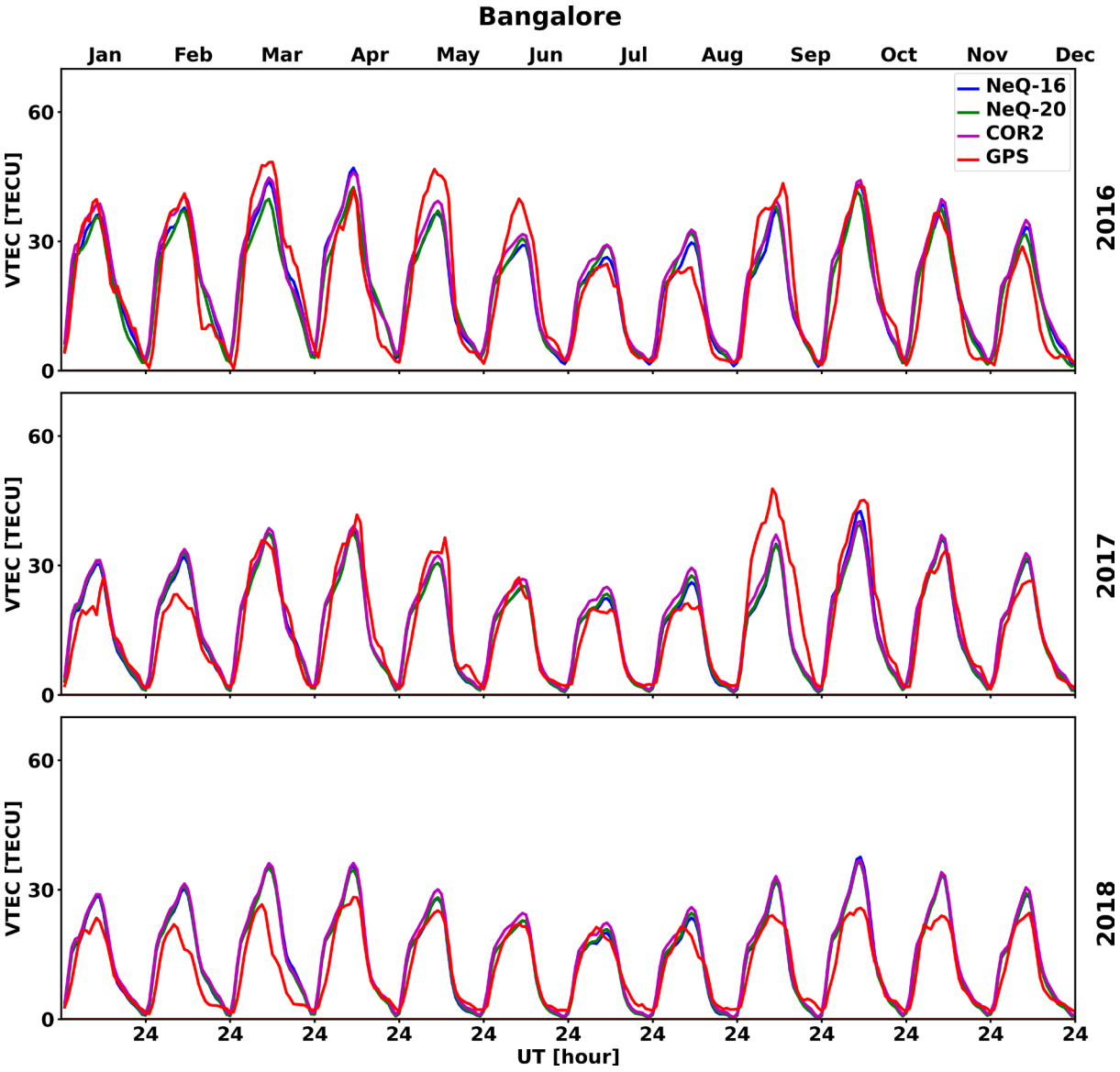

Figure 2. Diurnal variation of hourly TEC averaged over each month from GPS and three topside options (NeQ-16, NeQ-20, COR2) from IRI-2016 and IRI-2020 over Bangalore during 2016-2018.

3.2 Seasonal Variation of TEC and dTEC

Here, the comparison between the diurnal variation of hourly TEC data calculated over one year for three seasons from the GPS receiver and three topside options of IRI-2016 and IRI-2020 at Varanasi station and IGS station Bangalore is discussed. For better comprehension, we have discussed the seasonal variation of TEC and deviation in TEC between the model and GPS (dTEC), defined as (model TEC-GPS TEC) over both stations in a single plot for each year. In Figs. 3-5, the solid lines represent the variation of TEC as a function of UT, whereas the deviation of model-estimated TEC from GPS TEC (dTEC) is displayed as scatter points with lines. The left column shows the TEC variation for Varanasi, and the right column exhibits the same for Bangalore. The seasons are written along

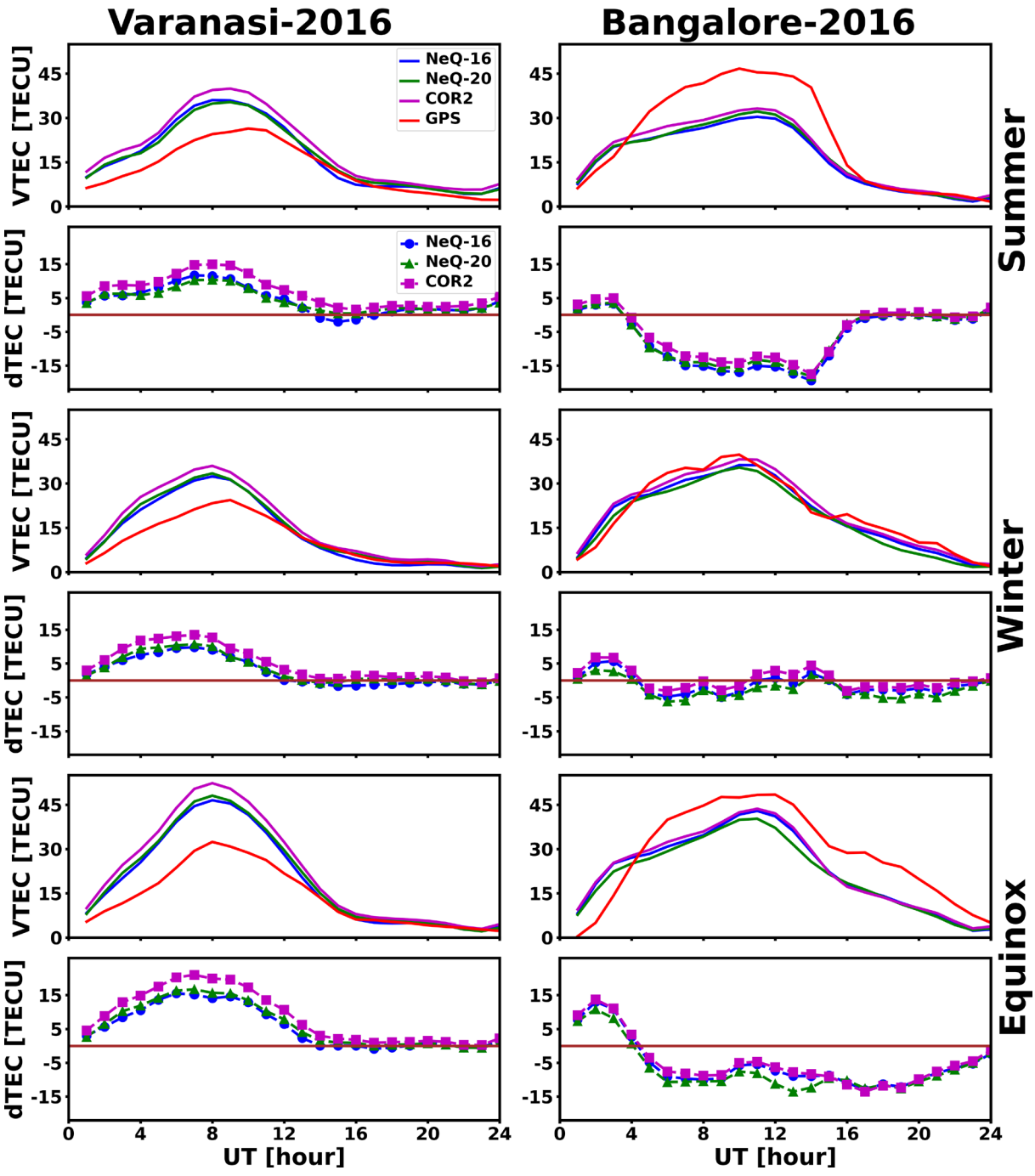

Figure 3. Diurnal variation of hourly TEC averaged over each season (summer, winter, and equinox) for GPS and three topside options (NeQ-16, NeQ-20, COR2) during the year 2016 over Varanasi (left column) and Bangalore (right column) with differences in TEC (IRI model TEC – GPS TEC).

the right vertical axis of each set of figures (TEC and dTEC). In Figs. 3-5, the overall pattern of TEC variation from both the data sets (GPS and Modeled) exhibits a steady increase from sunrise to noontime maximum, then falls to attain a minimum after sunset. The overall TEC variation trend can be categorized into the build-up region, the daytime peak region, and the decay region. The observed trend in the seasonal variation of TEC follows the characteristic pattern typical to the low-latitude ionospheres. For Varanasi (see the left columns of Figs. 3-5), the sharp buildup and steep decay regions result in a narrow peak between 07 UT and 09 UT for all the seasons. In contrast, a broader peak between 09 and 11 UT is observed in the seasonal variation of TEC over Bangalore (see the right columns of Figs. 3-5).

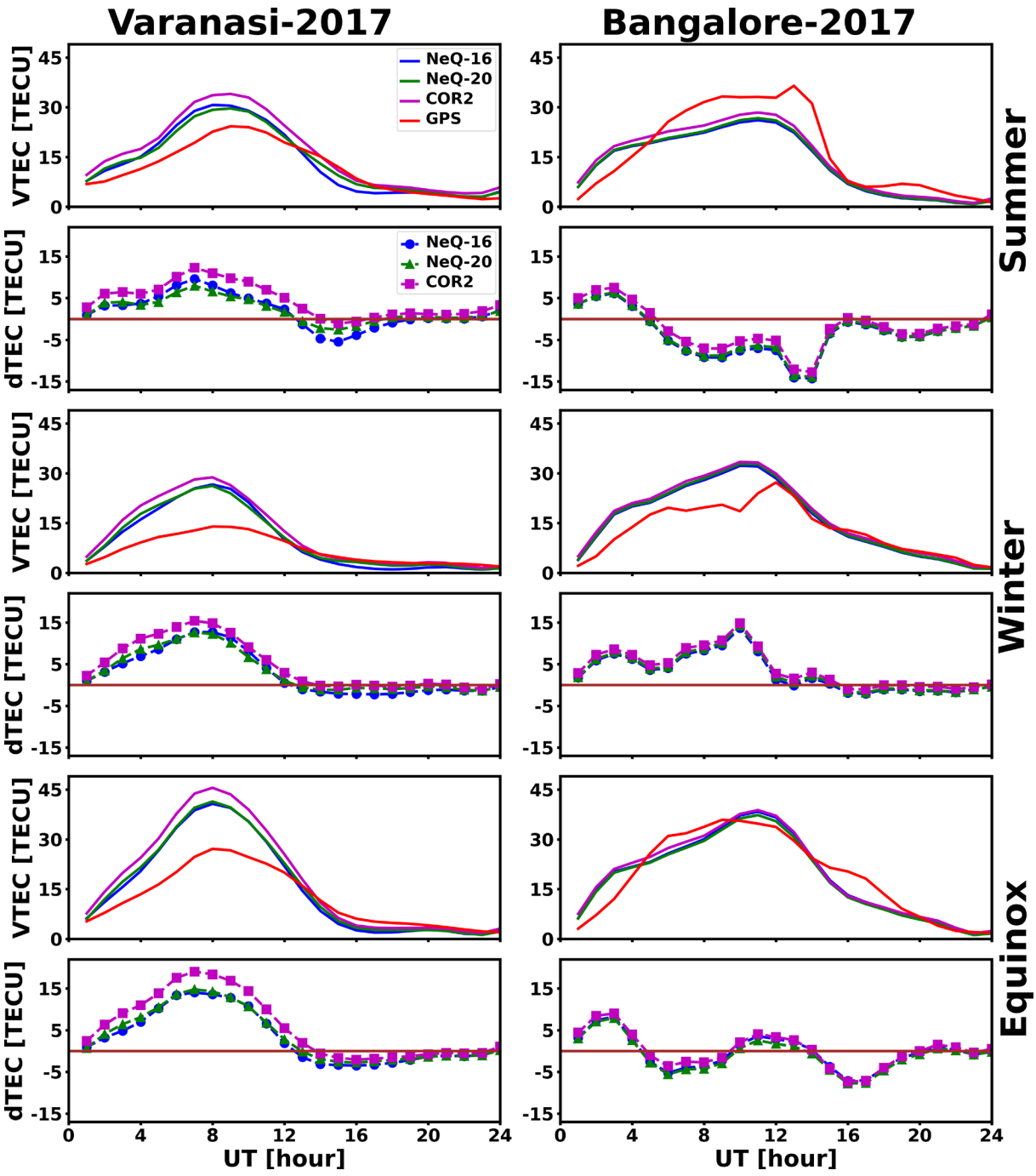

Figure 4. Diurnal variation of hourly TEC averaged over each season (summer, winter, and equinox) for GPS and three topside options (NeQ-16, NeQ-20, COR2) during the year 2017 over Varanasi (left column) and Bangalore (right column) with differences in TEC (IRI model TEC – GPS TEC).

Figure 3 shows the maximum TEC for the models and GPS for 2016 in the Equinox season over Varanasi and Bangalore. However, the GPS TEC is almost flat as compared to the modeled TEC during Equinox season over Bangalore resulting in very high discrepancy by the models as shown in the right column of Fig. 3. High discrepancy (overestimation) between the model TEC and the GPS observation is also seen over Varanasi between 01 UT and 16 UT. The highest overestimation (dTEC ~10 TECU) by all the topside options is found in the equinox during noontime over Varanasi. In contrast to the former behavior, the model underestimates GPS between 05 UT to 24 UT (dTEC ~−12 TECU). During the summer season, all the topside options overestimate the GPS TEC throughout the whole day over Varanasi, whereas overestimation and underestimation are both observed over Bangalore.

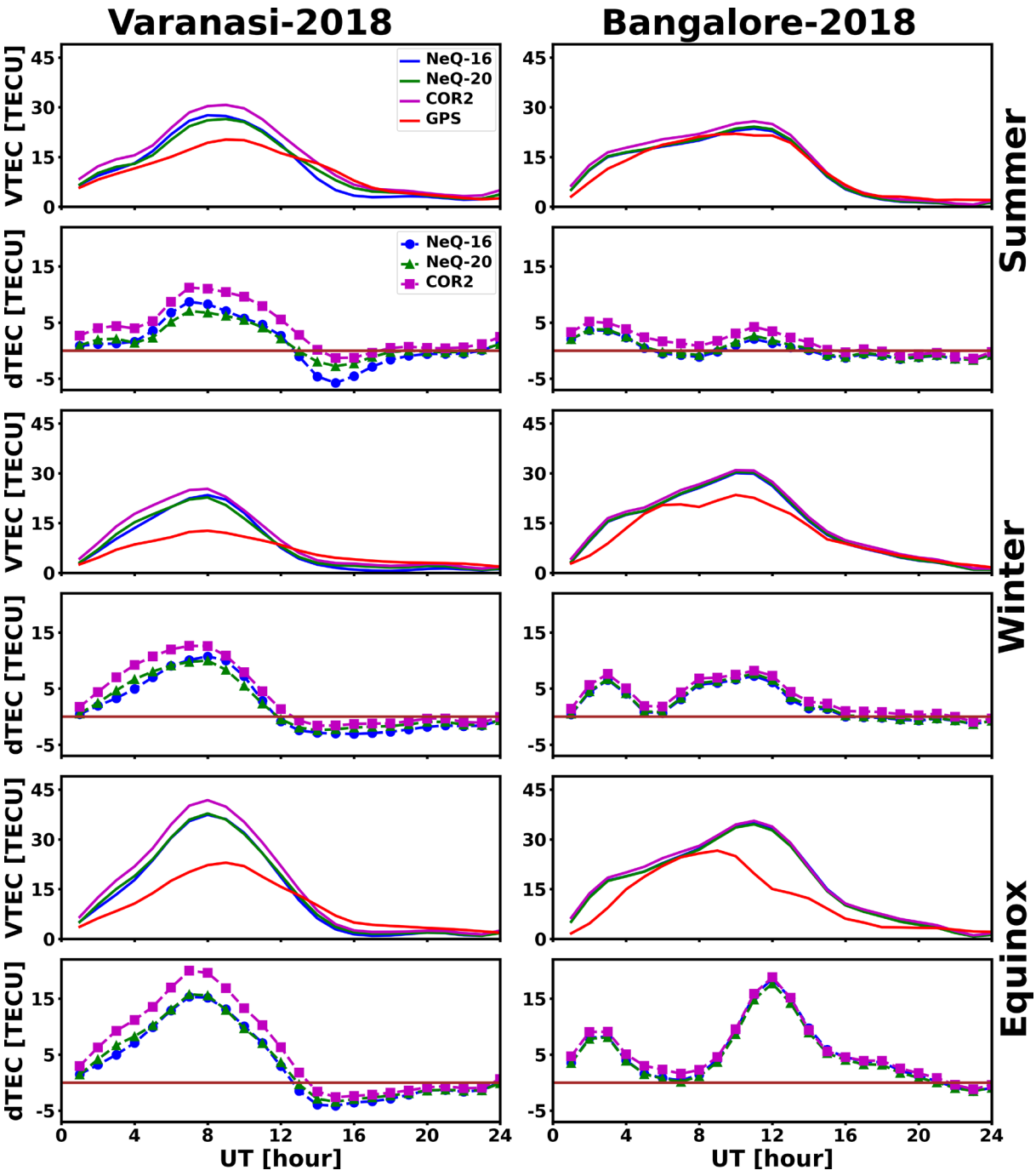

Figure 5. Diurnal variation of hourly TEC averaged over each season (summer, winter, and equinox) for GPS and three topside options (NeQ-16, NeQ-20, COR2) during the year 2018 over Varanasi (left column) and Bangalore (right column) with differences in TEC (IRI model TEC – GPS TEC).

Overestimation and underestimation by the modeled TEC over both stations are mainly observed during the daytime. Between 16 UT and 24 UT, the model estimation closely matches the GPS observation over both stations. All the topside options show good agreement (dTEC ~2 TECU) with GPS during the winter season over Bangalore for the entire day (01 UT-24 UT). However, the modeled TEC matches the GPS observation only from 13 UT to 24 UT over Varanasi during the Winter. Overall, the behavior of three topside options, NeQ-16, NeQ-20, and COR2, are closely identical over near equatorial and EIA regions during 2016.

Figure 4 shows the maximum TEC for the models and GPS for 2017 in the Equinox season over Varanasi and Bangalore. For 2017, all topside options exhibit similar behavior over Varanasi in all three seasons. The model-topside options overestimate the GPS TEC during 01 UT-12 UT with maximum overestimation observed in equinox season (dTEC ~20 TECU), whereas the model TEC matches the GPS TEC during 13 UT to 24 UT. The maximum diurnal TEC is found in the equinox season for both GPS and models. Figure 4 clearly shows that the TEC variation over Bangalore is flat compared to that over Varanasi, and the diurnal maximum TEC occurs later (~9 UT-11 UT) than in Varanasi. All three topside options show good performance in predicting GPS TEC during equinox season throughout the whole day (01 UT-24 UT) over Bangalore, whereas the model TEC overestimates and underestimates during winter (dTEC ~14 TECU) and summer (dTEC ~−14 TECU), respectively. The dTEC curve shows a pattern dCOR2 > dNeQ-16 & dNeQ-20 over Varanasi. On the other hand, dCOR2 ≈ dNeQ-16 & dNeQ-20 over Bangalore. This observation suggests that the newly added COR2 option of IRI-2020 has lower prediction accuracy over Varanasi than Bangalore in 2017.

Figure 5 exhibits the seasonal variation of modeled and GPS-derived TEC and dTEC for 2018 over Varanasi and Bangalore. For Varanasi, the overall trend of the TEC and dTEC variation is similar to the seasonal variation observed in 2016 and 2017, as shown in Fig. 3 and Fig. 4. In particular, during the summer season, the modeled TEC follows the GPS TEC over Bangalore. In contrast, GPS TEC is overestimated by all the topside options between 03 UT and 12 UT over Varanasi (dTEC ~10 TECU). The dTEC value for the COR2 option is slightly greater than the NeQ-16 and NeQ-20. A similar pattern was observed for two other seasons over Varanasi. The discrepancy between model prediction and GPS observation is highest during daytime hours for Varanasi. However, Bangalore does not show any common pattern in GPS observation, whereas three topside options exhibit dual peak patterns in diurnal variation for all seasons. The maximum overestimation is found in the equinox season (dTEC ~18 TECU). Deviation of model-derived TEC from GPS TEC in summer was observed over both stations.

3.3 Yearly Variation of dTEC

Figure 6 represents the prediction discrepancy between the hourly mean of model-estimated TEC and the GPS-derived TEC averaged over each year in terms of dTEC values over Varanasi and Bangalore for 2016, 2017, and 2018. Over Varanasi, the dTEC of all the topside options (NeQ-16, NeQ-20, and COR2) follows a common pattern for all the study years. They show an overestimation between 1 and 12 UT with a maximum dTEC value of 15 TECU for the COR2 topside option, followed by a good agreement for the rest of the time (13-24 UT). Another point to be noted is that the COR2 topside option exhibits a higher overestimation of GPS TEC compared to the other two topside options. In contrast to Varanasi, the dTEC of all the topside options over Bangalore does not follow a consistent pattern over the three study years. For the 2016 study year, all the topside options underestimates (negative dTEC value) the GPS TEC for the whole day, except between 1 and 4 UT. The maximum dTEC varies between ±10 TECU. For 2017, all the topside options mostly overestimate the GPS TEC during the daytime (1-12 UT) with the exception between 4 and 8 UT, where a good agreement is observed. During the nighttime (12-24 UT), all the topside options slightly underestimate the GPS TEC between 12 and 20 UT, followed by an accurate prediction for the rest of the nighttime. For 2018, all the topside options show good agreement with the GPS TEC for all the time, except during 1-4 UT and 8-16 UT when they overestimate the GPS TEC.

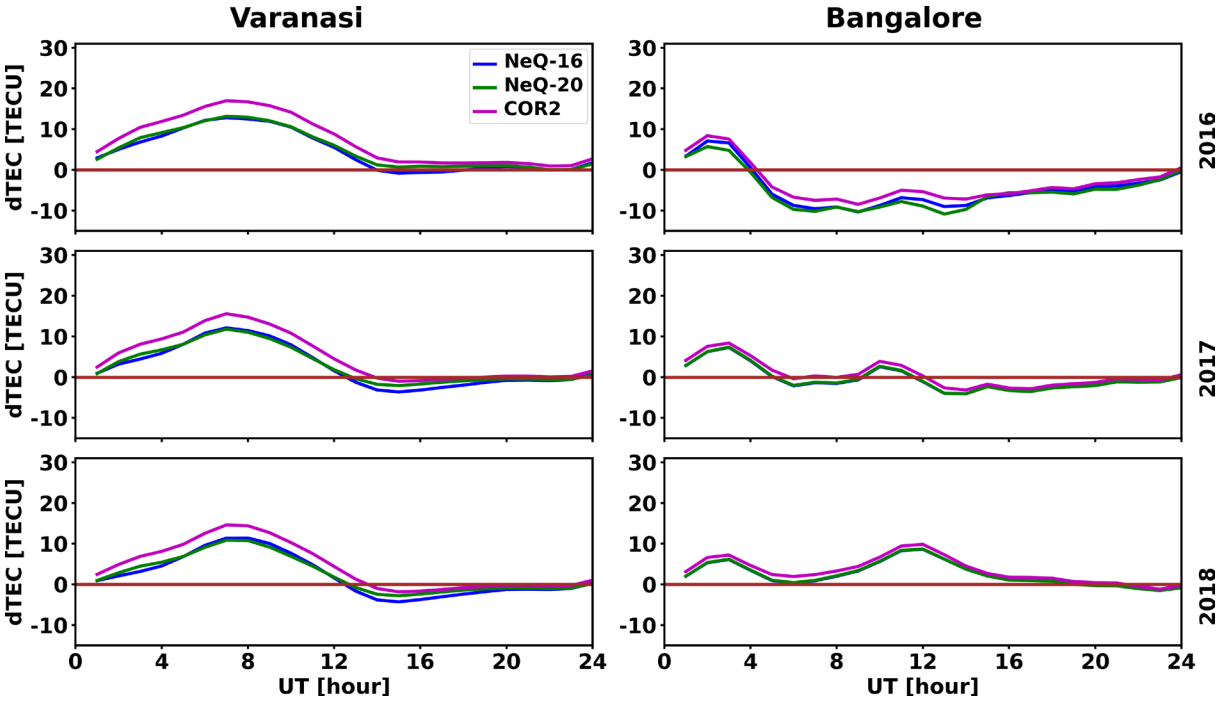

Figure 6. Diurnal variation of yearly averaged hourly dTEC (IRI model-GPS) values for three topside options (NeQ-16, NeQ-20, COR2) over Varanasi and Bangalore during 2016-2018.

3.4 Observation of Winter Anomaly (WA)

Another perspective to compare the performance of the models in predicting the GPS-TEC is to calculate the Winter anomaly (WA) phenomenon. Typically, the ionospheric ionization level in winter is lower than in summer. The phenomenon of a higher level of ionization in winter than in the summer is known as the Winter anomaly (Huang and Cheng, 1996). Generally, the winter anomaly is a mid-latitude phenomenon. Therefore, in this study, the difference of TEC between June and December of each year was taken to observe the WA over Varanasi, as shown in Fig. 7. GPS-TEC, as well as all the topside options of IRI-model TEC, are taken to evaluate the model performance. In Fig. 7, the positive bar implies the absence of WA, whereas the negative bar indicates WA.

Figure 7 shows the comparison of WA between all topside options and GPS over Varanasi. All the topside options accurately predict the GPS observation of WA for all the years. WA is absent over the whole study period. Interestingly, the COR2 option shows a higher value than the rest of the topside options.

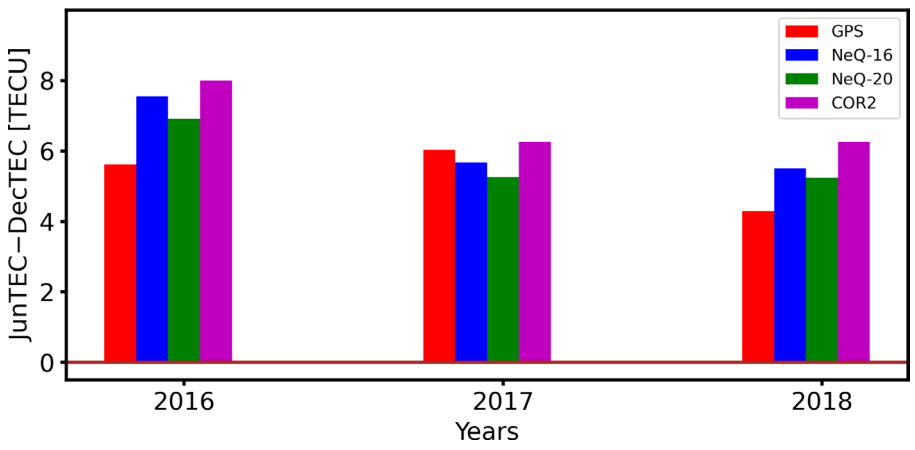

Figure 7. Anomaly in TEC (June TEC – December TEC) using GPS and IRI model over Varanasi for different years (2016-2018).

3.5 Observation of Equinoctial Asymmetry (EA)

Equinoctial Asymmetry (EA), first reported by Titheridge (1973) over the Northern and Southern hemispheres, is the phenomenon in which TEC values in the vernal equinoctial month (March) and spring equinoctial month (September) of a year are different. To investigate the EA during our observation period of 2016-2018 over Varanasi and Bangalore, the difference between the mean TEC of March and September of each year was calculated, and the values are reported in Table 1. The difference is taken for both GPS and the three topside options to validate the prediction performance of the IRI model. The positive value indicates that the March equinox TEC dominates over the September equinox.

TEC, whereas the negative value indicates the vice versa. EA is consistently observed every year of our whole study period. From our analysis, during 2016 and 2017, GPS and model performance concluded that the March equinox is more powerful than the September equinox over Varanasi, and the model shows good agreement with GPS. In Bangalore in 2017, all the topside options failed to predict GPS observations.

Table 1. Equinoctial asymmetry in TEC (March TEC – September TEC) using GPS and IRI model (NeQ-16, NeQ-20, COR2) over Varanasi and Bangalore for different years (2016-2018).

Stations	Years	GPS	NeQ-16	NeQ-20	COR2
Varanasi	2016	3.01	4.00	4.74	5.18
	2017	0.03	1.20	1.26	1.64
	2018	1.35	1.60	1.62	2.13
Bangalore	2016	5.90	7.50	3.96	6.16
	2017	-7.00	4.00	3.42	2.76
	2018	1.50	4.70	3.66	3.59

3.6 Correlation analysis between Model and GPS TEC

Figure 8 shows the comparison between the GPS TEC and the TEC data predicted by the model for all three topside options. The vertical axis represents the topside option data, whereas the horizontal axis indicates the GPS data. The solid line indicates the least-squares fitting to the data using Eq. (5). The correlation coefficient for each topside option, calculated using Eq. (3) for a total of $N = 1728$ data, is shown in the inset of each panel of Fig. 8. Overall, all the topside options show similar predicting ability with correlation coefficient around 0.87 ± 0.01.

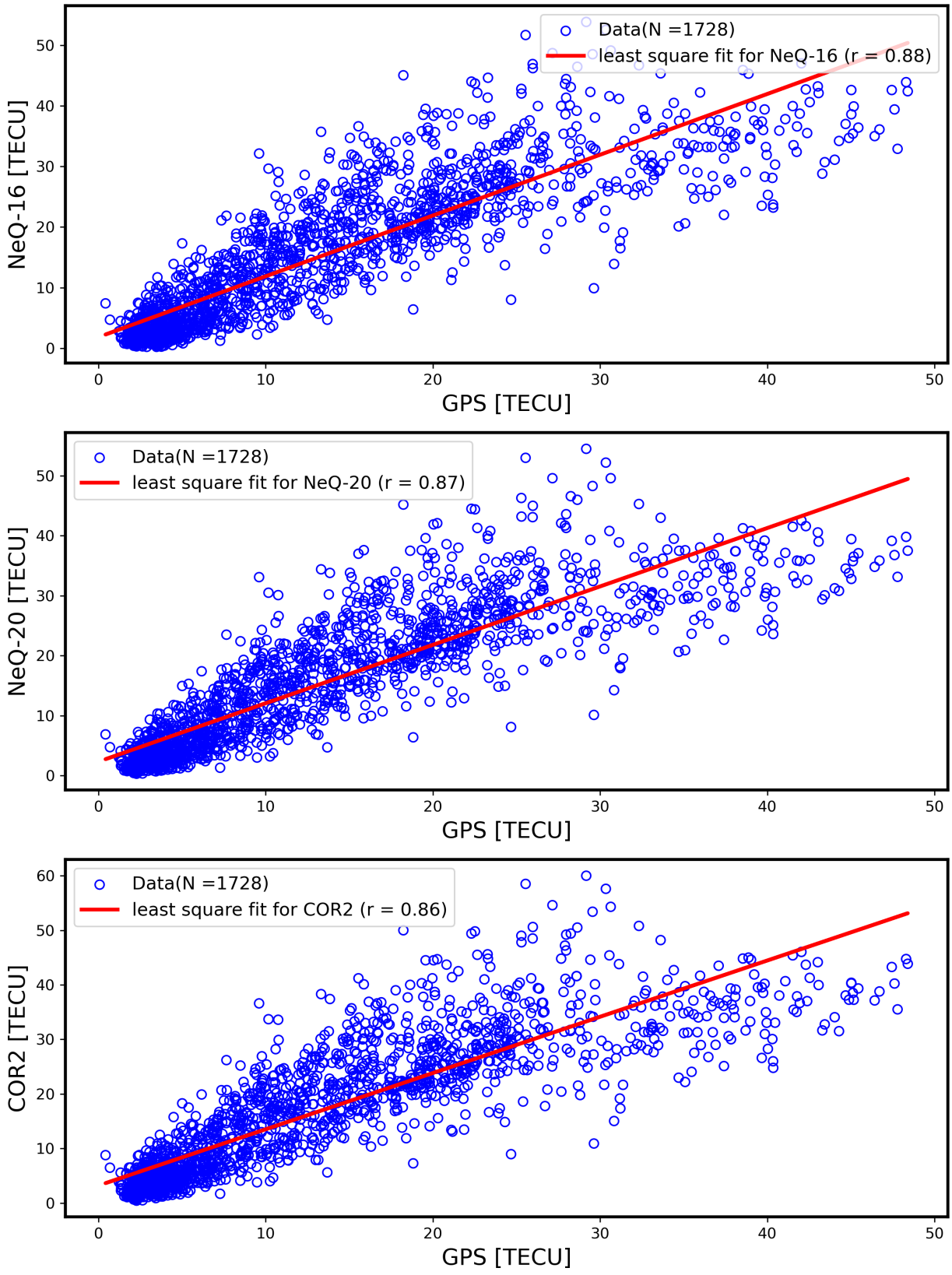

Figure 8. Comparison of GPS TEC and model-TEC derived from Ne-Quick topside options of IRI-2016 (top) and IRI-2020 (middle) and COR2 of IRI-2020 (bottom). The correlation coefficient was calculated as 0.88, 0.87, and 0.86 from top to bottom using N = 1728 data points.

3.7 Performance of the IRI models during geomagnetic storms

Figure 9 represents the performance of NeQ-16, NeQ-20, and COR2 options in predicting the hourly GPS TEC during four major geomagnetic storms recorded in our study period (2016-18). The number of recorded major storms and their intensity is very low, as our study focuses on the IRI performance in predicting the TEC during the solar minimum period. The storms are indicated by the disturbance storm time (Dst) index, which indicates the ring current of the Earth's magnetosphere. The duration of the storm is indicated in the Dst profile. In Fig. 9,

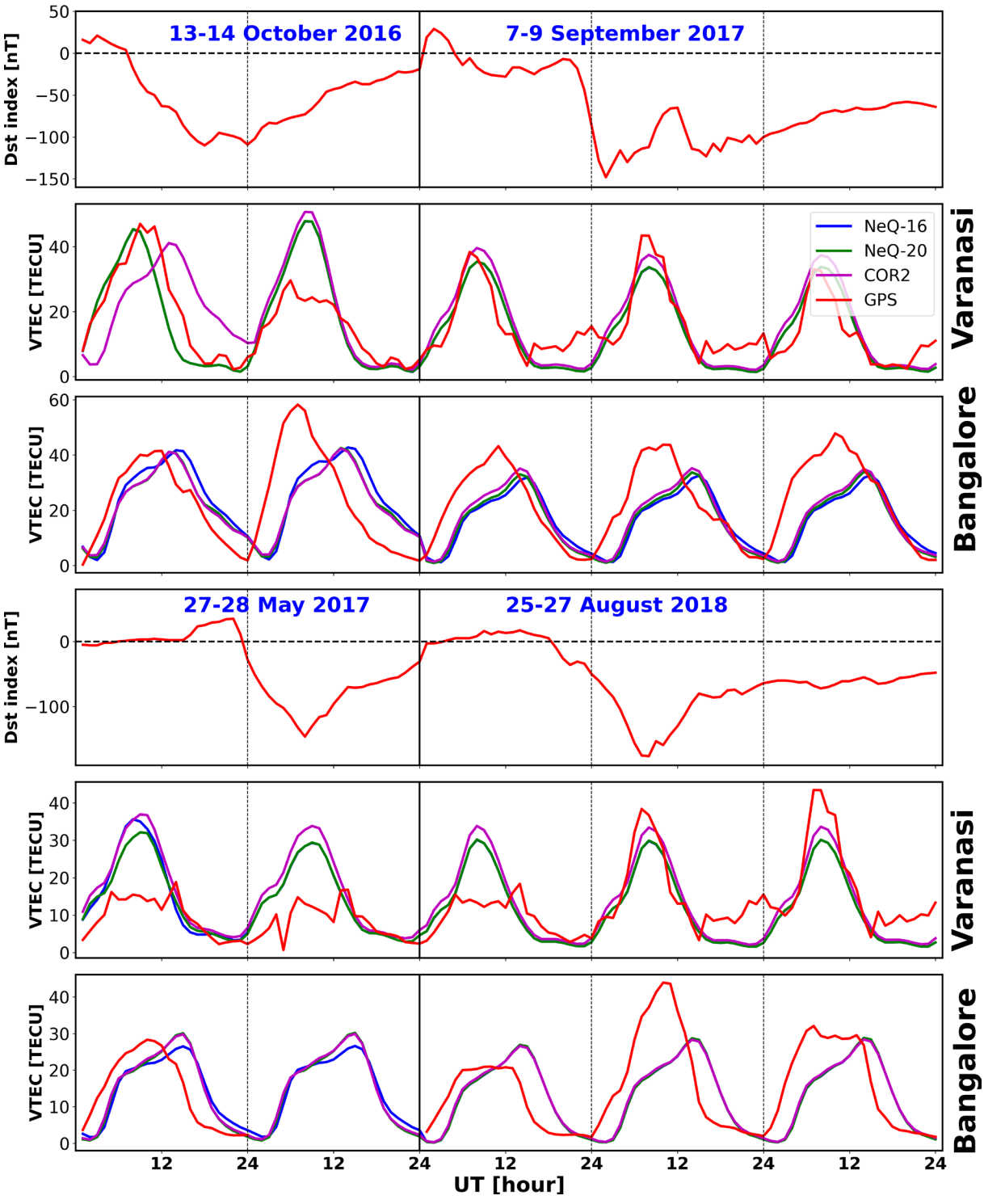

Figure 9. Diurnal variation of hourly mean TEC for GPS and three topside options (NeQ-16, NeQ-20, COR2) during four geomagnetic storms over Varanasi and Bangalore.

the consecutive rows following each Dst profile show the comparison between the GPS TEC and topside option TEC for Varanasi and Bangalore, respectively. The station names are written along the right vertical axis. The first three rows indicate the Dst index and the comparison of model and GPS TEC for the storms that occurred during the period 13-14 October 2016 (Min. Dst. = −110 nT) and 7-9 September 2017 (Min. Dst = −148 nT) over Varanasi and Bangalore. Whereas the last three rows indicate the same for the storms that occurred during the period 27-28 May 2017 (Min. Dst. = −146 nT) and 25-27 August 2018 (Min. Dst. = −110 nT). For all the storms during our study over both stations, the performance of all three topside options is poor in terms of predicting the GPS TEC. Specifically, the time of diurnal TEC maximum of the Model TEC does not match the GPS TEC, resulting in a difference in the TEC pattern for the models and the GPS TEC. Qualitatively, the prediction of the GPS TEC of Varanasi by all the topside options is poorer than that of Bangalore.

4. Discussion

TEC is a significant parameter in ionospheric physics for radio wave communication and navigation systems. Two processes mainly regulate TEC over equatorial and low-latitude EIA regions: first, the electron production by photoionization and loss of electrons by recombination with neutral atoms due to solar radiation, and second, the transportation of plasma via the fountain effect (Panda et al., 2015). Therefore, the variation of TEC over any region is mainly attributed to Solar radiation. The diurnal variation of TEC is due to the rotation of the Earth around its tilted axis (Liu and Chen, 2009), whereas the rotation of the Earth around the Sun results in seasonal variation of TEC.

Our study shows the mutual comparison of the forecasting performance of widely used empirical models IRI-2016 (NeQ-16) and its latest version IRI-2020 (NeQ-20 and COR2) using ground-based GPS-observations in terms of diurnal and seasonal behavior of TEC, the difference between the model estimation and GPS observation, winter anomaly, and equinoctial asymmetry during the descending phase 2016-2018 of 24^{th} solar cycle over EIA region Varanasi and the near equatorial region Bangalore. Overall, GPS observation, as well as IRI models (both versions), follow a similar pattern as the morning rise, noontime maximum, and afternoon decay in diurnal variation of TEC for different months and seasons of a year (cf. Figs. 1-5). However, in our analysis (monthly and seasonal variation), it has been observed that both IRI models overestimate during daytime and underestimate during nighttime over Varanasi and Bangalore. IRI models do not explicitly account for the electrodynamic processes (like $\mathbf{E} \times \mathbf{B}$ drifts) that control the development and strength of the EIA. As a result, the model often underestimates or overestimates the anomaly crests, leading to inaccuracies in TEC predictions, particularly in low-latitude regions where the EIA dominates the ionospheric structure.

Typically, the three topside options taken in our study (NeQ-16, NeQ-20, and COR2) compute the TEC (electron density) by considering the height of the ionosphere in the range between 60 and 2000 km, whereas the GPS TEC is measured by satellites orbiting at a much higher altitude (approximately 20,200 km). Therefore, the topside options expect an overestimation or underestimation in predicting the GPS TEC values. It was observed from the seasonal variation of TEC and dTEC analysis (Figs. 3-5) that the highest overestimation by the models with three topside options was found during noontime. The possible reason for the discrepancy (overestimation) is the decrease in electron density in the ionosphere, especially in the F-layer over the equatorial and low-latitude regions. At noon, solar radiation is at its peak, resulting in an increased photoionization rate. However, a simultaneous increase in the plasma drift velocity and horizontal transport of the plasma on both sides of the equator leads to a dip in electron density in the F-layer (Bilitza and Reinisch, 2008). At the near equatorial station, the prenoon peak in the diurnal variation of TEC is associated to the photoionization process whereas, afternoon peak is related to the F-layer drift and diffusion along the magnetic field lines (Martyn,1955; Rao, 1966). On the other hand, the contribution from the plasmasphere that is situated above 2000 km in the measurement of GPS-TEC during the nighttime increases by up to 60% as reported by Yizengaw et al. (2008). Therefore, the underestimations by the model during the nighttime are attributed to the exclusion of plasmaspheric contribution in TEC computation, observed by other researchers (Jethva et al., 2022; Chakraborty et al., 2014; Patel et al., 2019). The previous versions of the IRI-2020 model did not take the plasmaspheric contribution. According to Bilitza and Xiong (2021) and Bilitza et al. (2022), a correction in plasmaspheric contribution is incorporated in the IRI-2020 model. During our study period, nighttime underestimation by IRI-2020 is noticed over both stations for NeQ and COR2, which suggests more improvements are needed by incorporating more satellite data in the topside formulation of the model.

The seasonal variation of TEC, winter anomaly, and equinoctial asymmetry are due to the variation of solar radiation over the Earth's surface throughout the year. In our study, it has been observed that the mean GPS TEC in summer is greater than that in Winter in all the study years except in 2017 over Bangalore. This typical TEC seasonal variation is attributed to several factors, such as solar radiation variation due to the tilt of Earth's axis in its orbits around the Sun, geomagnetic activity such as solar storms and geomagnetic storms, temperature variation between the two seasons, and ionospheric dynamics, etc. The appearance of winter anomalies in 2017 may be explained in terms of compositional changes of neutral wind. The neutral winds are generated due to unequal heating of the two hemispheres (Balan et al., 1997). Due to uneven heating of the two hemispheres, the transport of neutral constituents from the summer to the winter hemisphere makes the O/N_2 ratio larger in the winter hemisphere than the same in the summer hemisphere. This recommends that the possibility of recombination in the winter hemisphere is weaker as compared to the summer hemisphere, which results in a relatively higher electron concentration in the winter hemisphere (Rishbeth and Setty, 1961; Torr and Torr, 1973; Galav et al., 2011). Another possibility of the formation of winter anomaly is due to the change of neutral wind direction. The meridian component of wind blowing opposite to plasma diffusion from the summer hemisphere into the winter hemisphere is expected to reduce crest values at the summer solstice (Wu et al., 2004; 2008). During the solar minimum period, the winter anomalies are disappeared, as reported by previous works (Lin et al., 2007; Balan et al., 2013). Dieu Nibigira et al. (2021) reported the absence of WA during 2016-2018 over both hemispheres. Moreover, the equinox season exhibits the highest occurrence of TEC over both stations, irrespective of the study year. This is mainly attributed to the position of the sub-solar point around the equatorial region in the equinox season, leading to high photoionization during the equinox compared to the solstices. Due to this, the eastward electric field enhances the equatorial electrojet, influencing the TEC disparity over low-latitude regions.

In addition, another important point is that the NeQ-16, NeQ-20, and COR2 topside options exhibit similar characteristics in each perspective (diurnal, monthly, seasonal, WA, EA) to estimate GPS measurements in our study period over both stations. The quantitative analysis of the correlation coefficient between model TEC and GPS TEC and RMSE of the dTEC (Model TEC – GPS TEC) are reported for three topside options used in the present study. From the yearly averaged dTEC plot (see Fig. 7), the degree of overestimation by the COR2 topside options is slightly higher than the other two (NeQ-16 and NeQ-20) over Varanasi during 2016-2018. As seen from Table 2, the highest overall RMSE for the COR2 option is 8.16 for Varanasi. From Fig. 7, it is also seen that the prediction patterns by both Ne-Quick options are similar throughout the whole time (01-24 UT) and between 01 UT-12 UT; overestimations are observed for all the years over Varanasi, whereas overestimations are seen for a few hours over Bangalore. In 2016, underestimation by all the topside options was mostly observed from 4 UT to 24 UT. In 2017, prediction discrepancy is very less (dTEC ~7 TECU), implying good performance of the three topside options. No underestimation is found by the model in 2018 over Bangalore. The performance of COR2 is better than the other two options over Bangalore with the lowest overall RMSE = 6.02 (see Table 2).

From Table 2, the yearly RMSE values of the NeQ-16 topside option display the lowest value than the NeQ-20 and COR2 options over Varanasi, suggesting better predictability during our study period. In addition, the yearly RMSE of the COR2 topside shows the lowest value over Bangalore in 2016 and 2017, implying better accuracy of COR2 during our study period. In 2018, NeQ-20 gave the lowest value (4.63). No significant improvements are observed in NeQ-20 compared to the previous version NeQ-16 over two regions. Schreiber et al. (2024) reported similar results over low latitudes. Their study reported the better accuracy of the Ne-Quick option at low latitudes. This better predictability of the Ne-Quick topside option may be attributed to its computation ability of electron density contribution from both ionospheres as well as plasmasphere using a semi-Epstein layer function with a height-dependent thickness (i.e. scale height) parameter (Radicella and Leitinger, 2001; Coisson et al., 2006; Bilitza et al., 2006; Bilitza and Reinisch, 2008). On the other hand, the new topside option COR2 provides a smooth transition from the topside ionosphere to the plasmasphere. According to Bilitza et al. (2022), prediction of electron density by the COR2 option is a function of the peak electron density of the F2 layer, altitude, geomagnetic latitude, the plasma frequency of the F2 layer, the height of that peak, and the one-year (365 days) running mean of the solar flux at 10.7 cm, and a correction term associated with the altitude, modified dip latitude, and local time.

Over the near equatorial region (Bangalore), the prediction of GPS TEC by all the topside options is equivalent (RMSE ~6). From the calculation of overall RMSE, calculated for three years, the COR2 among all the topside options predicts the GPS TEC slightly better with the lowest RMSE = 6.02 compared to both Ne-Quick options (RMSE = 6.22).

In contrast to Bangalore, both Ne-Quick options predict the GPS TEC (with RMSE ~6.1) better than the COR2 option (8.16) over the EIA region (Varanasi). IRI models are developed and regularly updated based on data from

Table 2. Root mean squared error (RMSE) of seasonal averaged dTEC values over Varanasi and Bangalore for three topside options (NeQ-16, NeQ-20, and COR2) during 2016-2018.

Station	Year	Season	NeQ-16	NeQ-20	COR2
Varanasi	2016	Summer	5.88	5.36	8.08
		Winter	4.77	5.25	6.89
		Equinox	9.04	9.82	12.27
		Total	**6.80**	**7.13**	**9.37**
	2017	Summer	4.32	3.49	5.87
		Winter	5.94	5.85	7.43
		Equinox	6.89	7.12	9.34
		Total	**5.81**	**5.69**	**7.68**
	2018	Summer	4.13	3.21	5.49
		Winter	5.06	4.80	6.29
		Equinox	7.15	7.28	9.46
		Total	**5.59**	**5.36**	**7.28**
	Overall		**6.09**	**6.11**	**8.16**
Bangalore	2016	Summer	10.38	9.67	8.80
		Winter	3.07	3.64	2.90
		Equinox	8.90	9.62	8.67
		Total	**8.09**	**8.15**	**7.33**
	2017	Summer	6.41	6.15	5.49
		Winter	5.20	5.49	5.96
		Equinox	3.94	4.04	4.09
		Total	**5.28**	**5.30**	**5.24**
	2018	Summer	1.57	1.66	2.43
		Winter	3.58	3.78	4.43
		Equinox	7.26	6.87	7.53
		Total	**4.76**	**4.63**	**5.24**
	Overall		**6.22**	**6.22**	**6.02**

various sources such as ionosonde, radar data, rocket measurements, and satellite data. Being the data-dependent model, the overestimation or underestimation by the model is related to the fact that IRI models are simulated with very little data from low latitude (equatorial) regions (Bilitza et al., 2022; Marew et al., 2023).

To compare the performance of NeQ-16, NeQ-20, and COR2 models in terms of predictability of GPS TEC over two stations for a total of 3 study years, a quantitative statistical analysis (least square fit with correlation coefficient calculation) was performed over N = 1728 data points. The results are displayed in Fig. 8. All the topside options perform equivalently well with a very high correlation coefficient of 0.86 for COR2, 0.87 for NeQ-20, and 0.88 for NeQ-16. These findings are also supported by the station-wise RMSE of dTEC as listed in Table 2. In summary, we found no major difference in the prediction ability of all the topside options for our study period over the near equatorial and EIA regions.

In addition to the IRI model prediction during the quiet time, the storm time performance of the IRI model was investigated during four major storms recorded during our study period, as shown in Fig. 9. The deviation between the GPS and the model prediction in terms of RMSE and correlation coefficient is shown in Table 3.

Table 3. Root mean squared error (RMSE) of hourly mean dTEC values and correlation coefficient during geomagnetic storm days over Varanasi and Bangalore for three topside options (NeQ-16, NeQ-20, and COR2) during 2016-2018.

Topside option	RMSE		Correlation Coefficient
	Varanasi	Bangalore	
NeQ-16	7.72	12.80	0.67
NeQ-20	7.52	12.42	0.70
COR2	9.23	12.06	0.66

In Fig. 9 and Table 3, all the topside options fail to reproduce the GPS observation in disturbed geomagnetic conditions. COR2 option shows maximum RMSE with 9 TECU and 12 TECU over Varanasi and Bangalore, respectively, which are very high compared to the quiet day RMSE values. Further, the correlation coefficient of all the topside options is around ~0.73 for storm time, which is lower than the quiet day correlation coefficient values. The results of higher RMSE and lower correlation coefficient during the storm time, compared to the quiet day, suggest that the IRI model fails to predict the GPS TEC. This may be because the IRI model does not incorporate the geomagnetic storm conditions. Therefore, to forecast the storm time TEC correctly by IRI models, the storm parameters such as Dst, Ey, and Bz are required to be included in the models. These improvements in the IRI models will enhance prediction ability of TEC resulting in enhance signal accuracy and reliability in satellite communication and GPS navigation by reducing ionospheric delay and positioning errors. They also strengthen space weather forecasting by providing better insight into ionospheric responses to solar and geomagnetic activity.

5. Summary and Future Prospects

In this article, we have represented a comparative study of the ionospheric TEC prediction performance of IRI models (IRI-2016 and IRI-2020) using the ground-based GPS measurements over the EIA region Varanasi and the near equatorial region Bangalore during the descending phase of the 24th solar cycle, 2016-2018. To understand the forecasting performance of the IRI models, rigorous statistical analysis, such as the comparison of diurnal, monthly, seasonal, and annual TEC variation between the model and GPS, RMSE of the seasonal dTEC variation, and correlation coefficient calculation using the least squares regression analysis method, was performed. The significant findings of the study are as follows:

– The trend of diurnal TEC variation from GPS and Models follows a similar pattern as morning rise, daytime maximum, and is followed by afternoon decay for all the study years over both stations, but the peak TEC

occurs earlier (by approximately 2 hrs.) for Varanasi than Bangalore. Moreover, the daytime peak TEC values for GPS as well as IRI models show a nearly sinusoidal trend with peaks in April and October and valley regions in January-April, May-August, and September-December.
- The seasonal variation analysis shows that the maximum and minimum TEC from GPS and IRI models occur in the equinox and winter, respectively, for both stations in all the study years. In addition, a narrow peak was observed in Varanasi, whereas in Bangalore, a broad peak was found for all the study years.
- For Varanasi, all topside options of IRI-2016 and IRI-2020 predict the GPS winter anomaly results.
- Equinoctial asymmetry was observed in GPS measurements in all the study years over both stations. In addition, all the topside options of the IRI models correctly predict the observed equinoctial asymmetry results.
- The RMSE analysis of dTEC shows that the forecasting performance of the NeQ-16 topside option over Varanasi is most accurate, with the lowest RMSE of 6.09, whereas the prediction capability of COR2 options is found superior (RMSE = 6.02) to the other two topside options over Bangalore.
- Overall, the correlation coefficient using least-squares regression analysis for the three topside options shows that the prediction accuracy of the NeQ-16 is most accurate for the solar minima 2016-2018, with the highest correlation coefficient of 0.88.
- All topside options show poor prediction performance with high RMSE around 12 TECU for Bangalore compared to Varanasi (RMSE ~8 TECU) and overall correlation coefficient around 0.73 for forecasting the GPS-TEC during storm conditions.

In summary, our study focuses on the forecasting performance of the recent topside options of the IRI model during the low solar activity years over near equatorial and EIA stations. However, the equatorial and low-latitude ionosphere is an important region with various physical processes, such as the fountain effect, plasma bubbles formation, and equatorial electro-jet, to name a few. In addition, generally, the high solar activity periods exhibit frequent intense geomagnetic storms, which may impact the forecasting performance of the IRI models during the high geomagnetically active period. Therefore, many future studies focusing on the comparison between the recently developed IRI-2020 models and the ground-based GPS TEC over more stations situated across the equatorial and low-latitude stations during high and low solar activity periods will help the evaluation of the forecasting performance of the models. The authors expect the findings of the present study will be helpful to the research community in the field of ionospheric physics as a reference for validating the significantly improved recent IRI models for the study of TEC characteristics.

Data availability statement. IRI Data can be downloaded at: https://kauai.ccmc.gsfc.nasa.gov/instantrun/iri. IGS data can be downloaded at: https://igs.org/data/daily.

Acknowledgements. The work is partially supported by the Institute of Imminence (IoE) Program (Scheme No: 6031) of BHU, Varanasi. MM is thankful for the financial support from UGC. The IRI-modelled TEC data are freely available at the IRI website: ccmc.gsfc.nasa.gov.

References

Appleton, E. V. (1946). Two anomalies in the ionosphere, Nature 157, 691-691. doi:10.1038/157691a0.

Amaechi, P. O., E. O. Oyeyemi, A. O. Akala, M. Kaab et al. (2021). Comparison of ionospheric anomalies over African equatorial/low-latitude region with IRI-2016 model predictions during the maximum phase of solar cycle 24, Adv. Space Res., 68, 3, 1473-1484, doi:10.1016/j.asr.2021.03.040.

Bailey, G. J., N. Balan and Y. Z. Su (1997). The Sheffield University plasmasphere ionosphere model review, J. Atmos. Solar-Terr. Phys., 59, 1541-1552, doi:10.1016/S1364-6826(96)00155-1.

Balan, N., Y. Otsuka and S. Fukao (1997). New aspects in the annual variation of the ionosphere observed by the MU Radar, Geophys. Res. Lett., 24, 18, 2287-2290. doi:10.1029/97gl02184.

Balan, N., P. K. Rajesh, S. Sripathi, S. Tulasiram et al. (2013). Modeling and observations of the north–south ionospheric asymmetry at low latitudes at long deep solar minimum, Adv. Space Res. 52, 375-382.

Bilitza D., B. W. Reinisch, S. M. Radicella, S. Pulinets et al. (2006). Improvements of the International Reference Ionosphere model for the topside electron density profile, Radio Sci., 41, 05, 1-8. RS5S15, doi:10.1029/2005RS003370.

Bilitza, D. and B. W. Reinisch (2008). International reference ionosphere 2007: improvements and new parameters, Adv. Space Res. 42, 4, 599-609, doi:10.1016/j.asr.2007.07.048.

Bilitza, D., B. Reinisch and J. Lastovicka (2008). Progress in observation-based ionospheric modeling. Space Weather, 6, S02002, doi:10.1029/2007SW000359.

Bilitza, D., S. A. Brown, M. Y. Wang, J. R. Souza et al. (2012). Measurements and IRI model predictions during the recent solar minimum, J. Atmos. Solar-Terr. Phys., 86, 99-106, doi:10.1016/j.jastp.2012.06.010.

Bilitza, D., D. Altadill, Y. Zhang, C. Mertens et al. (2014). The international reference ionosphere 2012 – a model of international collaboration, J. Sp. Weather Sp. Clim. 4, A07, doi:10.1051/swsc/2014004.

Bilitza, D., D. Altadill, V. Truhlik and V. Shubin (2017). International Reference Ionosphere 2016: From ionospheric climate to real-time weather predictions, Space Weather, 15, 2, 418-429, doi:10.1002/2016SW001593.

Bilitza, D. and C. Xiong (2021). A solar activity correction term for the IRI topside electron density model, Adv. Space Res., 68, 5, 2124-2137, doi:10.1016/j.asr.2020.11.012.

Bilitza, D., M. Pezzopane, V. Truhlik, D. Altadill et al. (2022). The International Reference Ionosphere model: A review and description of an ionospheric benchmark, Rev. Geophys., 60, 4, e2022RG000792, doi:10.1029/2022RG000792.

Chakraborty, M., S. Kumar, B. K. De and A. Guha (2014). Latitudinal characteristics of GPS derived ionospheric TEC: a comparative study with IRI 2012 model, Ann. Geophys., 57, 5, A0539, doi:10.4401/ag-6438.

Chauhan, V. and O. P. Singh (2010). A morphological study of GPS-TEC data at Agra and their comparison with the IRI model, Adv. Space Res., 46, 280-290, doi:10.1016/j.asr.2010.03.018.

Chaurasiya, S. K., K. Patel, S. Kumar and A. K. Singh (2023). Analysis of GPS-TEC and IRI model over equatorial and EIA stations during solar cycle 24, Adv. Space Res., 72, 11, 4882-4895. doi:10.1016/j.asr.2023.09.014.

Coïsson, P., S. M. Radicella, R. Leitinger and B. Nava (2006). Topside electron density in IRI and NeQuick: Features and limitations, Adv. Space Res, 37, 5, 937-942, doi:10.1016/j.asr.2005.09.015.

De Dieu Nibigira, J., G. Sivavaraprasad and D. V. Ratnam (2021). Performance analysis of IRI-2016 model TEC predictions over Northern and Southern Hemispheric IGS stations during the descending phase of solar cycle 24, Acta Geophys., 69, 4, 1509-1527, doi:10.1007/s11600-021-00618-1.

Endeshaw, L. (2020). Testing and validating IRI-2016 model over Ethiopian ionosphere, Astrophys. Space Sci., 365, 3, 49, doi:10.1007/s10509-020-03761-1.

Galav, P., S. Sharma and R. Pandey (2011). Study of simultaneous penetration of electric fields and variation of total electron content in the day and night sectors during the geomagnetic storm of 23 May 2002, J. Geophys. Res. 116, A12324, doi:10.1029/2011JA017002.

Gatica-Acevedo, V. J., M. A. Sergeeva, O. A. Maltseva, J. A. Gonzalez-Esparza et al. (2024). TEC variations and IRI-2016, IRI-2020 and IRI-Plas performance in Mexico, Adv. Space Res., doi:10.1016/j.asr.2024.03.046.

He, R., M. Li, Q. Zhang and Q. Zhao (2023). A Comparison of a GNSS-GIM and the IRI-2020 Model Over China Under Different Ionospheric Conditions, Space Weather, 21, 10, e2023SW003646, doi:10.1029/2023SW003646.

Huang, Y. N. and K. Cheng (1996). Solar cycle variation of equatorial ionospheric anomaly in total electron content in the Asian region, J. Geophys. Res. 101,24513-24520.

Jethva, C., M. S. Bagiya and H. P. Joshi (2022). On the GPS TEC variability for full solar cycle and its comparison with IRI-2016 model, Astrophys. Space Sci., 367, 8, 80, doi:10.1007/s10509-022-04112-y.

Kumar, S., S. Priyadarshi, S. Gopi Krishna and A. K. Singh (2012). GPS-TEC variations during low solar activity period (2007-2009) at Indian low latitude stations, Astrophys. Space Sci., 339, 165-178, doi:10.1007/s10509-011-0973-6.

Kumar, S., K. Patel and A. K. Singh (2016). TEC variation over an equatorial and anomaly crest region in India during 2012 and 2013, GPS solut., 20, 617-626, doi:10.1007/s10291-015-0470-4.

Kumar, S. (2020). North-South asymmetry of equatorial ionospheric anomaly computed from the IRI model, Ann. Geophys., 63, 3, DM330-DM330, doi:10.4401/ag-8324.

Lee, H.-B., G. Jee, Y. H. Kim and J. S. Shim (2013). Characteristics of global plasmaspheric TEC in comparison with the ionosphere simultaneously observed by Jason-1 satellite, J. Geophys. Res.: Space Phys., 118, 2, 935-946.

Lin, C. H., J. Y. Liu, T. W. Fang, P. Y. Chang et al. (2007). Motions of the equatorial ionization anomaly crests imaged by FORMOSAT-3/COSMIC, Geophys. Res. Lett. 34, L19101, doi:10.1029/2007 GL030741.

Liu, L. and Y. Chen (2009). Statistical analysis of solar activity variations of total electron content derived at Jet Propulsion Laboratory from GPS observations, J. Geophys. Res.: Space Phys., 114, A10, doi:10.1029/2009JA014533.

Marew, H., A. Agmas and T. Mersha (2024). Performance evaluation for vertical TEC predictions over the East Africa and South America: IRI-2016 and IRI-2020 versions, Adv. Space Res., 73, 1, 698-715, doi:10.1016/j.asr.2023.09.055.

Martyn, D. F. (1955). The physics of the ionosphere. The Physical Society, London, 260.

Nava, B., P. Coïsson and S. M. Radicella (2008). A new version of the NeQuick ionosphere electron density model, J. Atmos. Solar-Terr. Phys., 70, 1856-1862, doi:10.1016/j.jastp.2008.01.015.

Ogwala, A., E. O. Somoye, S. K. Panda, O. Ogunmodimu et al. (2021). Total electron content at equatorial and low-, middle-and high-latitudes in African longitude sector and its comparison with IRI-2016 and IRI-PLAS 2017 models, Adv. Space Res., 68, 5, 2160-2176, doi:10.1016/j.asr.2020.07.013.

Ogwala, A., O. J. Oyedokun, O. Ogunmodimu, A. O. Akala et al. (2022). Longitudinal variations in equatorial ionospheric TEC from GPS, global ionosphere map and international reference ionosphere-2016 during the descending and minimum phases of solar cycle 24, Universe, 8, 11, 575, doi:10.3390/universe8110575.

Ogwala, A., F. F. Akinbuli, S. K. Panda, P. Jamjareegulgarn et al. (2024). On the variations in equatorial and low-latitude GPS-TEC and assessment of NeQuick-2, IRI-2016 and IRI-2020 models in the African longitude during solar cycle 24-25, Adv. Space Res., doi:10.1016/j.asr.2024.05.031.

Panda, S. K., S. S. Gedam and S. Jin (2015). Ionospheric TEC variations at low latitude Indian region. Satellite Positioning-Methods, Models and Applications, Tech-Publisher, Rijeka, Croatia, 149-174, doi:10.5772/59988.

Patel, N. C., S. P. Karia and K. N. Pathak (2019). Evaluation of the improvement of IRI-2016 over IRI-2012 at the India low-latitude region during the ascending phase of cycle 24, Adv. Space Res., 63, 6, 1860-1881, doi:10.1016/j.asr.2018.10.008.

Patari, A., B. Paul and A. Guha (2021). Statistics of GPS TEC at the northern EIA crest region of the Indian subcontinent during the solar cycle 24 (2013-2018): comparison with IRI-2016 and IRI-2012 models, Astrophys. Space Sci., 366, 5, 46, doi:10.1007/s10509-021-03950-6.

Priyadarshi, S., W. P. Syam, A. A. G. Roqué and A. P. Conesa (2025). On the development of HARMONY Machine learning (ML) IONO demonstrator, Adv. Space Res., 75, 1, 966-987, doi:10.1016/j.asr.2024.09.042.

Radicella, S. M. and R. Leitinger (2001). The evolution of the DGR approach to model electron density profiles, Adv. Space Res., 27, 1, 35-40, doi:10.1016/S0273-1177(00)00138-1.

Rathore, V. S., S. Kumar and A. K. Singh (2015). A statistical comparison of IRI TEC prediction with GPS TEC measurement over Varanasi, India, J. Atmos. Solar-Terr. Phys., 124, 1-9, doi:10.1016/j.jastp.2015.01.006.

Rama Rao, P. V. S., S. Gopi Krishna, K. Niranjan and D. S. V. V. D. Prasad (2006). Temporal and spatial variations in TEC using simultaneous measurements from the Indian GPS network of receivers during the low solar activity period of 2004 and 2005, Ann. Geophys., 24, 12, 3279-3292, doi:10.5194/angeo-24-3279-2006.

Rao, B. N. (1966). Control of equatorial spread-F by the F-layer height, J. Atmos. Terr. Phys., 28, 12, 1207-1217, doi:10.1016/S0021-9169(17)30067-3.

Rao, S. S., M. Chakraborty, S. Kumar and A. K. Singh (2019). Low-latitude ionospheric response from GPS, IRI and TIE-GCM TEC to Solar Cycle 24, Astrophys. Space Sci., 364, 1-14, doi:10.1007/s10509-019-3701-2.

Rishbeth, H. and C. S. G. K. Setty (1961). The F-layer at sunrise, J. Atmos. Terr. Phys. 20, 263-276, doi:10.1016/0021-9169(61)90205-7.

Rishbeth, H. (1972). Thermospheric winds and the F-region: a review, J. Atmos. Terr. Phys. 34, 1-47, doi:10.1016/0021-9169(72)90003-7.

Servan-Schreiber, N., M. Aggarwal, Y. Huang, M. Kang et al. (2024). Validation of the IRI-2020 model for the topside-plasmasphere using GNSS TEC measurements, Adv. Space Res., doi:10.1016/j.asr.2024.07.009.

Shahzad, R., M. Shah and A. Ahmed (2021). Comparison of VTEC from GPS and IRI-2007, IRI-2012 and IRI-2016 over Sukkur Pakistan, Astrophys. Space Sci., 366, 4, doi:10.1007/s10509-021-03947-1.

Sulungu, E. D. (2024). Performance of IRI 2016 model in predicting total electron content (TEC) compared with GPS-TEC over East Africa during 2019-2021, Sci. Rep., 14, 1, 10010, doi:10.1038/s41598-024-59624-0.

Tariq, M. A., M. Shah, M. Ulukavak and T. Iqbal (2019). Comparison of TEC from GPS and IRI-2016 model over different regions of Pakistan during 2015-2017, Adv. Space Res., 64, 3, 707-718, doi:10.1016/j.asr.2019.05.019.

Titheridge, J. E. (1974). Changes in atmospheric composition inferred from ionospheric production rates, J. Atmos. Terr. Phys., 36, 7, 1249-1257, doi:10.1016/0021-9169(74)90111-1.

Torr, M. R. and D. G. Torr (1973). The seasonal behaviour of the F2-layer of the ionosphere, J. Atmos. Terr. Phys., 35, 12, 0-2251, doi:10.1016/0021-9169(73)90140-2.

Wu, C. C., C. D. Fry, K. Liou and C. L. Tseng (2004). Annual TEC variation in the equatorial anomaly region during the solar minimum: September 1996-August 1997, J. Atmos. Terr. Phys., 66, 3-4, 199-207, doi:10.1016/j.jastp.2003.09.017.

Wu, C. C., C. D. Fry, K. Liou, S. J. Shan et al. (2008). Variation of ionospheric total electron content in Taiwan region of the equatorial anomaly from 1994 to 2003, Adv. Space Res., 41, 4, 611-616, doi:10.1016/j.asr.2007.06.013.

Yang, Y., L. Liu, X. Zhao, T. Han et al. (2024). A quantitative analysis of latitudinal variation of ionospheric total electron content and comparison with IRI-2020 over China, Adv. Space Res., 73, 7, 3808-3817, doi:10.1016/j.asr.2023.05.040.

Yizengaw, E., M. B. Moldwin, D. Galvan, B. A. Iijima et al. (2008). Global plasmaspheric TEC and its relative contribution to GPS TEC, J. Atmos. Solar-Terr. Phys., 70, 11-12, 1541-1548, doi:10.1016/j.jastp.2008.04.022.

***CORRESPONDING AUTHOR: Abhay KUMAR SINGH**,

Banaras Hindu University, Institute of Science, Department of Physics, Varanasi, U.P., India-221005

e-mail: singhak@bhu.ac.in